ОПТИЧЕСКИЙ ЖУРНАЛ. 2023. Том 90. № 8. С. 96–110
OPTICHESKII ZHURNAL. 2023. V. 90. № 8. Pp. 96–110
Научная статья
Research Article
Оптический журнал
Оптическое приборостроение и метрология
Optical materials and technology
DOI: 10.17586/1023-5086-2023-90-08-96-110

Rain attenuation analysis of radio over free space optics system considering diverse regions

Sanmukh Kaur[1]✉, Jasleen Kaur[2]

Amity School of Engineering & Technology, Amity University, Noida, India

[1]*sanmukhkaur@gmail.com* *https://orcid.org/0000-0002-1750-5684*
[2]*jasleen_kaur@outlook.in* *https://orcid.org/0000-0001-5576-9149*

Abstract

Subject of study. In post-pandemic world connectivity plays an important role and is one of the biggest assets for economy. Radio over free space optics is one of the most in-demand wireless communication technology solutions for 5G deployment in the upcoming era of a fast-moving world. **Purpose of the work:** To analyze the performance of radio over free space optics link under the rain weather conditions. **Method.** In this research, diverse geographical rain conditions for different terrains of India have been analyzed for monsoon months using Marshall and Palmer rain attenuation model. **Main results.** Based on the real rain rate data analysis, it has been observed that an effective link range of up to 4 km may be achieved with an acceptable signal/noise ratio and bit error rate of 20 dB and 10^{-9} respectively even for the coastal region with heavy rainfall. **Practical significance:** As rain is one of the dominant weather conditions affecting free space optics link, the proposed model employing orthogonal frequency-division multiplexing based QAM-64 and PSK-16 modulation schemes at a data rate 20 Gbps is able to limit the degrading effects of the channel.

Keywords: radio over free space optics, signal/noise ratio, bit error rate,rain attenuation

For citation: Sanmukh Kaur, Jasleen Kaur. Rain attenuation analysis of radio over free space optics system considering diverse regions (Анализ ослабления сигнала в радиосистемах на основе беспроводной оптической связи в дождевых условиях с учётом климатических особенностей региона) [In English] // Opticheskii Zhurnal. 2023. V. 90. № 8. P. 96–110. http://doi.org/10.17586/1023-5086-2023-90-08-96-110

OCIS codes: 060.2605, 060.4510, 140.0140, 010.1300.

Анализ ослабления сигнала в радиосистемах на основе беспроводной оптической связи в дождевых условиях с учётом климатических особенностей региона

Sanmukh Kaur[1]✉, Jasleen Kaur[2]

Amity School of Engineering & Technology, Amity University, Noida, India

[1]*sanmukhkaur@gmail.com* *https://orcid.org/0000-0002-1750-5684*
[2]*jasleen_kaur@outlook.in* *https://orcid.org/0000-0001-5576-9149*

Аннотация

Предмет исследования. Пути совершенствования технологии передачи радио-приложений через системы беспроводной оптической связи как перспективного элемента 5G систем.

Цель работы. Повышение производительности радиосистем на основе беспроводной оптической связи в дождевых условиях. **Метод.** Анализ ослабления оптического излучения в дождевых условиях для различных районов Индии в течение муссонных месяцев с использованием модели Маршалла–Пальмера. **Основные результаты.** Установлено, что эффективная дальность связи до 4 км с частотой ошибок по битам не более 10^{-9} обеспечивается для прибрежного региона с обильными муссонными осадками при отношении сигнал шум не менее 20 дБ. **Практическая значимость.** Предлагаемая модель, использующая схемы квадратурной амплитудной модуляции QAM-64 и фазовой двоичной манипуляция PSK-16 на основе ортогонального мультиплексирования с частотным разделением при скорости передачи данных 20 Гбит/с, способна значительно уменьшить ослабление сигнала в системах беспроводной оптической связи вследствие негативного влияния дождевых условий.

Ключевые слова: радиосистемы на основе беспроводной оптической связи, отношение сигнал/шум, частота ошибок по битам, ослабление излучения в дождевых условиях

Ссылка для цитирования: SanmukhKaur, JasleenKaur. Rain attenuation analysis of radio over free space optics system considering diverse regions (Анализ ослабления сигнала в радиосистемах на основе беспроводной оптической связи в дождевых условиях с учётом климатических особенностей региона [на англ. языке] // Оптический журнал. 2023. Т. 90. № 8. С. 96–110. http://doi.org/10.17586/1023-5086-2023-90-08-96-110

Коды OCIS: 060.2605, 060.4510, 140.0140, 010.1300.

1. INTRODUCTION

The upcoming era of the communication system is expected to revolutionize different sectors like healthcare, manufacturing, data analysis, smart cities, automobiles, security services, etc. Next-generation communication services will allow faster and reliable transmission of data to meet the immense demands of internet connectivity and high-capacity links. Radio frequency (RF)communications have been widely deployed in indoor, space and terrestrial communication systems. With the increase in applications of RF communication, RF spectrum experiences congestion and becomes expensive to acquire. Industry and the research community have been putting several efforts for the enhancement of the capabilities of present wireless technologies and for developing latest ones for fulfilling emerging requirements [1–3].

With the increase in demand for high-speed data services in different geographical regions, more reliable and high bandwidth wireless connectivity is required. Radio over free space optics (RoFSO) is one of the most in-demand upcoming wireless communication technology approaches for the successful execution of next-generation 5G data services. It acts as an alternative technology to existing RF communication systems with a key advantage that it allows the distribution of RF signals at high bandwidth. It provides flexibility in wireless communications that may be deployed in different geographical terrains [4–7].

RoFSO link, despite many advantages, may experience severe degradations due to atmospheric turbulence. Different atmospheric conditions such as rain, fog, haze, etc. results in the fading and scattering of the transmitted information signal. Diverse geographical regions may experience different meteorological weather conditions in India resulting in attenuation in RoFSO channel causing degradation in the link performance. Rain is the significant contributor for transmission losses when operating frequency for FSO communication is above 5GHz. Wireless Signals can be affected by the rain, because droplets of water absorb the signal resulting in deterioration of overall signal strength. Rain is considered as one of the primary factors of RoFSO link performance degradation [8–10]. The precipitation maps are used to depict the distribution pattern of the rainfall over certain time periods and areas.

Orthogonal frequency-division multiplexing (OFDM) acts as an effective modulation technique in communication systems due to its high spectral efficiency as different OFDM subcarriers are completely overlapped. OFDM encodes digital data on multiple carrier frequencies and may be used for scenarios, where severe attenuation is caused by harsh weather conditions [11–13]. Quadrature amplitude modula-

tion (QAM) has achieved significant attention in wireless domain due to its capability in providing high speed data transmission with better received power and bandwidth efficiency. Phase shift keying (PSK) is another modulation technique, in which phase is changed to represent the data signal, and is also widely used in wireless communication applications [14]. These modulations are preferred choices and are more efficient for higher data rate optical wireless systems [5].

Deployment of 5G data services requires high-capacity links employing advanced modulation techniques for seamless wireless connections. RoFSO provides one of the best solutions for above mentioned requirements and for high-speed end of mile access applications with 5G communication. There is a necessity to enhance the connectivity, reliability and maintain link even during harsh weather conditions, including rain effects [15].

Different research studies have been conducted around the world to assess RoFSO system performance. In [16] Authors demonstrated the performance of RoFSO operating at 75Ghz using Mach Zehnder modulator (LiNb). OFDM based RoF system with DSP (Digital signal processor) has been employed to achieve 100 Gb/s bit rate. Performance of the system has been evaluated for coherent and direct detection systems considering both 16-PSK and 16-QAM modulation schemes. In [17] authors describe the transmission of OFDM radio signals using QAM encoding format over FSO channel link. The gamma-gamma distribution has been used to analyze the atmospheric turbulence effect for estimating the performance of the system. The authors have proposed an architecture for analysis of 2.4 GHz photonic antenna for RoF link in [18]. The performance of the system has been evaluated at data rate of 2.5 Gbps for fiber length of 50 km by employing 16-QAM modulation scheme. In [19] fog attenuation in hilly areas of India have been investigated with the help of the Kruse model with an average attenuation of 0.86 dB/Km at 1550 nm wavelength. The received signal has been analyzed for FSO link employing amplitude shift keying(ASK), PSK and duo binary return-to-zero (DRZ) modulation techniques. In [20] Authors presented 1280 Gbps hybrid fiber and FSO system with 32 channel DWDM (dense wavelength division multiplexing) and advanced modulation formats. The received signal degrades beyond FSO channel range of 1000 m, 800 m and 400 m for heavy fog, haze and rain weather conditions respectively. In [21] 320 Gbps, 32 channels hybrid fiber + FSO system has been evaluated by employing on-off keying modulation scheme. An acceptable bit error rate (BER) of 10^{-13} has been achieved up to 130 m transmission range under clear weather condition.

In this research we have proposed and analyzed RoFSO link for different geographical terrains such as plain, hilly, and coastal regions under the rain weather condition. The values of rain attenuations for diverse regions of India have been calculated for monsoon months of the years ranging from 2014 to 2020 using Marshall and Palmar model. The performance of the system has been evaluated by employing 64 QAM – OFDM and 16 PSK – OFDM modulation techniques in terms of bit error rate, signal-to-noise ratio and the received power for varying FSO link ranges.

Section II consists of rain rate analysis and calculation of rain attenuations for different topography of India and monsoon months respectively. The proposed RoFSO system and related equations are described in Section III. In section IV simulation results of the system models employing advanced modulation techniques have been discussed. Conclusion is given in the section V.

2. RAIN RATE AND ATTENUATION ANALYSIS

The rainfall rate for the diverse topography of India has been considered for RoFSO link analysis. Rainfall attenuations have been analyzed for three different regions, i.e. hilly (Uttarakhand), plain (Chandigarh), and coastal (Kerala) as depicted in Fig. 1.

Rainfall attenuation is the calculation of attenuation per unit length. The data for real time rainfall have been extracted from Meteorological Department of India. The rainy weather attenuations have been computed from the collected data for specific rain months of five years using rain attenuation model. Rainfall attenuations for different regions are using Marshal and Palmar model. The Rain attenuation values are determined by

$$\gamma\left(\frac{dB}{km}\right) = aR^b. \quad (1)$$

It uses the basic power law with a and b as power-law parameters. R is the rain rate in mm/hour. For Marshal and Palmer's model, the value for a is 0.365 and b is 0.63. The data for different rain rates for six years and four monsoon months have been collected for diverse different regions and have been analyzed using the statistical model.

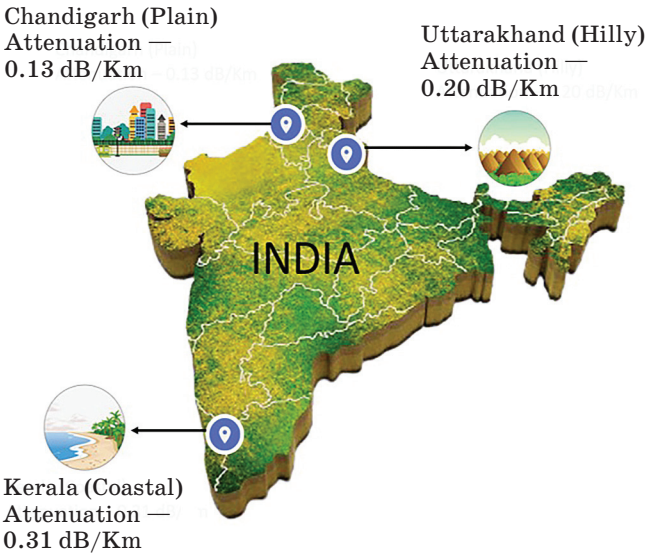

Fig. 1. Different geographical regions considered for RoFSO link analysis

Рис. 1. Географические регионы, рассматриваемые при анализе RoFSO связи

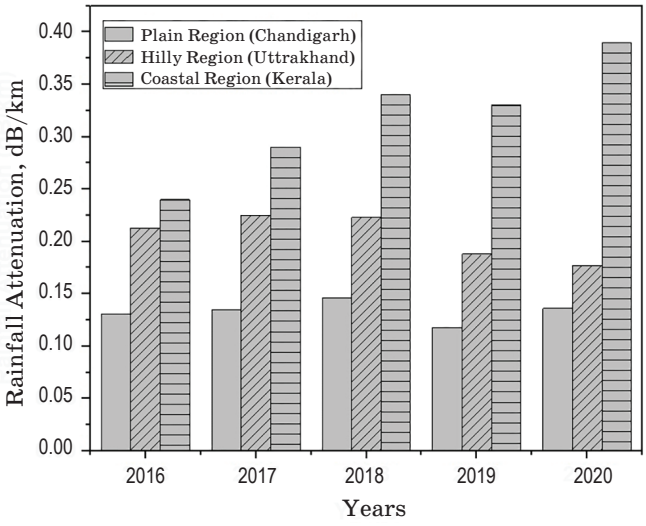

Fig. 2. Rainfall attenuation (dB/km) for diverse geographical regions

Рис. 2. Ослабление сигнала вследствие осадков (дБ/км) для различных географических регионов

Fig. 2 represents the rainfall attenuation for diverse geographical regions of India for the years 2016–2020 considering monsoon months. The rainfall attenuation is more in the coastal region and least in the plain region, whereas it is moderate for the hilly region. The maximum and minimum rainfall attenuations were experienced in the years 2018 and 2019 for coastal and plain regions respectively.

Table 1 and Fig. 3 depict the rain attenuation in dB/km of the plain region for the months June–September. The plain region (Chandigarh) experiences the maximum and minimum attenuations in the months of July and June respectively over the years 2016–2020. Rainfall attenuation for plain region ranges from 0.118 dB/km to 0.146 dB/km. The average rainfall attenuation of different months for different years has been calculated and the overall average attenuation value for plain region is predicted as 0.13 dB / Km.

Rain attenuation for monsoon months in the hilly region ranges from 0.077 dB/km to 0.35 dB/km, which is represented in Fig. 4 and Table 2. The hilly region (Uttarakhand) experiences the maximum and minimum rain attenuations in the months of June and September respectively over the years 2016–2020. The average rainfall attenuation of different months for the diverse years has been calculated and further the overall average attenuation value for hilly region is predicted as 0.20 dB/km.

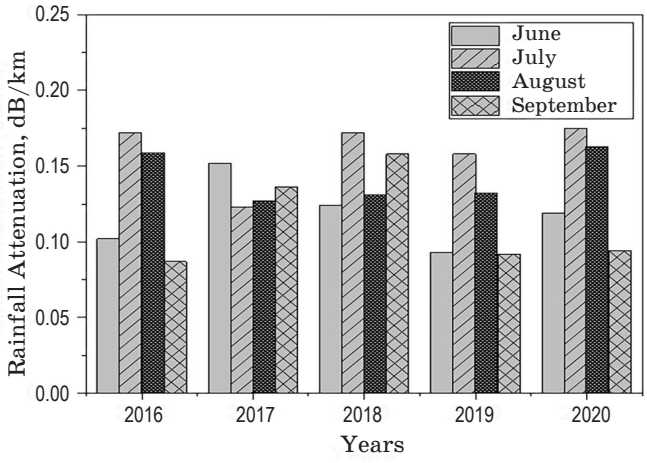

Fig. 3. Rainfall attenuation (dB/km) for plain region (Chandigarh)

Рис. 3. Ослабление сигнала вследствие осадков (дБ/км) для равнинного региона (Чандигарх)

Table 1. Rainfall attenuation in dB / km for plain region (Chandigarh)
Таблица 1. Ослабление сигнала вследствие осадков (дБ/км) для равнинного региона (Чандигарх)

Year Month	Rainfall attenuation in dB / km for plain region				
	June	July	August	September	Average
2016	0.102	0.172	0.159	0.087	0.131
2017	0.152	0.123	0.127	0.136	0.135
2018	0.124	0.172	0.131	0.158	0.146
2019	0.093	0.158	0.132	0.092	0.118
2020	0.119	0.175	0.163	0.094	0.136
Average rainfall attenuation					0.13

Table 2. Rainfall attenuation (dB/km) data for hilly region (Uttarakhand)
Таблица 2. Ослабление сигнала вследствие осадков (дБ/км) для холмистого региона (Уттаракханд)

Year Month	Rainfall attenuation in dB / km for plain region				
	June	July	August	September	Average
2016	0.325	0.314	0.239	0.198	0.213
2017	0.327	0.297	0.255	0.194	0.225
2018	0.309	0.268	0.291	0.207	0.223
2019	0.204	0.231	0.259	0.172	0.188
2020	0.285	0.262	0.263	0.074	0.177
Average rainfall attenuation					0.20

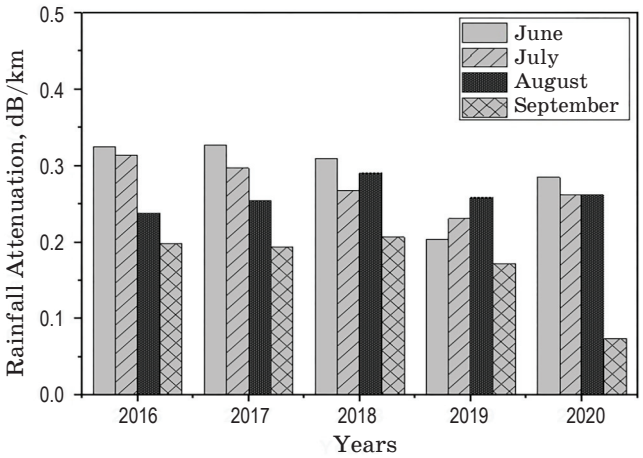

Fig. 4. Rainfall attenuation (dB/km) for hilly region (Uttarakhand)

Рис. 4. Ослабление сигнала вследствие осадков (дБ/км) для холмистого региона (Уттаракханд)

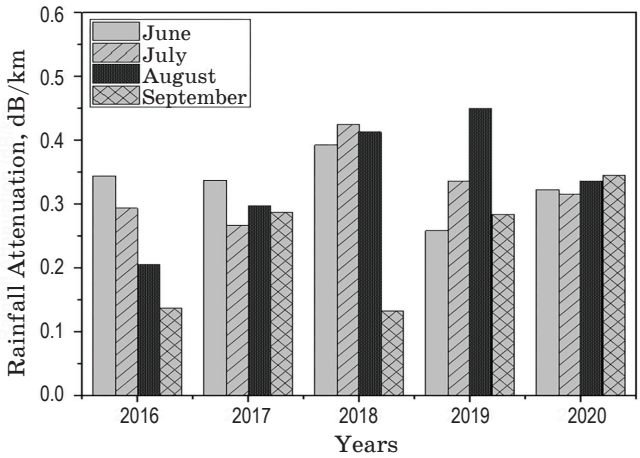

Fig. 5. Rainfall attenuation (dB/km) for coastal region (Kerala)

Рис. 5. Ослабление осадков (дБ/км) для приморского региона (Керала)

Figure 5 and Table 3 demonstrates the rain attenuations for coastal region, which ranges from 0.24 dB/km to 0.39 dB/km. The coastal region (Kerala) experiences the maximum and minimum rain attenuations in the months of August and September respectively over the years 2016–2020. The average rainfall attenuation of different months for the five years has been calculated and further the overall average attenuation value for hilly region is predicted as 0.31 dB/km.

Table 3. Rainfall attenuation (dB/km) data for coastal region (Kerala)
Таблица 3. Ослабление осадков (дБ/км) для приморского региона (Керала)

Year / Month	Rainfall attenuation in dB / km for coastal region				
	June	July	August	September	Average
2016	0.345	0.294	0.206	0.137	0.24
2017	0.338	0.267	0.298	0.288	0.29
2018	0.393	0.425	0.414	0.133	0.34
2019	0.259	0.336	0.451	0.284	0.33
2020	0.323	0.316	0.337	0.346	0.39
Average rainfall attenuation					0.31

The minimum and maximum values of the average rain attenuation of 0.13 and 0.31 dB/Km have been observed in the plain and coastal region respectively for a wavelength of 1550 nm. Hilly region experiences moderate average rain attenuation of 0.20 dB/ Km. The average rain attenuation values for diverse regions have been considered for further analysis of RoFSO system.

3. RoFSO SYSTEM MODEL

Here the link design parameters used for the analysis of the proposed RoFSO system have been discussed. OFDM has been used for the frequencies division as it improves the system performance resulting in the increment of transmission range. Spectral efficiency and BER performance of PSK and QAM improves and deteriorates respectively with the order of modulation [14]. We have chosen QAM-64 and 16-PSK based OFDM system for rain attenuation modelling analysis, so that the performance of the link may be investigated for higher order modulation schemes. The data signal is being processed by sequence generator for generating phase and quadrature signals with 1200 subcarriers. Low pass cosine roll-off filters have been used in shaping the pulses before the transmission. The signals from these filters are fed into two different Mach–Zehnder modulators (MZM). Continuous wave (CW) laser signal is applied to the lower MZM. The output of both the MZM is further combined using the power combiner. The FSO channel experiences the attenuation and scattering of the laser light. The receiver signal at the other end of the FSO channel is detected by a PIN photodiode and resultant electrical signal is applied to the quadrature demodulator. The signal is further filtered using low-power cosine roll-off filters and the output is fed to the OFDM demodulator. QAM detector detects the message signal and BER test set calculates the system performance by counting the number of errors. The system models of 64-QAM and 16-PSK based OFDM have been depicted in Fig. 6a and Fig. 6b respectively.

The total input current comprises of signal and noise. The current generated by the photodiode positive intrinsic negative (PIN) can be represented as follows:

$$I_{\mathrm{p}}(t) = r.(E_{\mathrm{sig}} + E_{\mathrm{ase}}(t))^2 + I_{\mathrm{d}} + I_{\mathrm{s}}(t) + I_{\mathrm{t}}(t), \quad (2)$$

where E_{sig} and E_{ase} represent the electric field components linked with the power at the input block and noise respectively. I_{d} and I_{t} refer to as dark current and thermal current respectively. I_{s} represents the random fluctuation of electric current. The frequency response of the photodiode PIN is determined by

$$\frac{I_{\mathrm{out}}}{I_{\mathrm{in}}} = \frac{1}{1+RC}, \quad (3)$$

where R is the load resistance and C refers to junction capacitance. The sensitivity of a PIN photodiode can be defined in terms of its noise equivalent power, where SNR = 1. The noise equivalent power (NEP) is calculated by

$$\mathrm{NEP} = \frac{\sqrt{\left(I^2 + I_S\right)} + \sqrt{I_t}}{\mathrm{Responsivity}} \frac{1}{\sqrt{\mathrm{Noise\ bandwidth}}}. \quad (4)$$

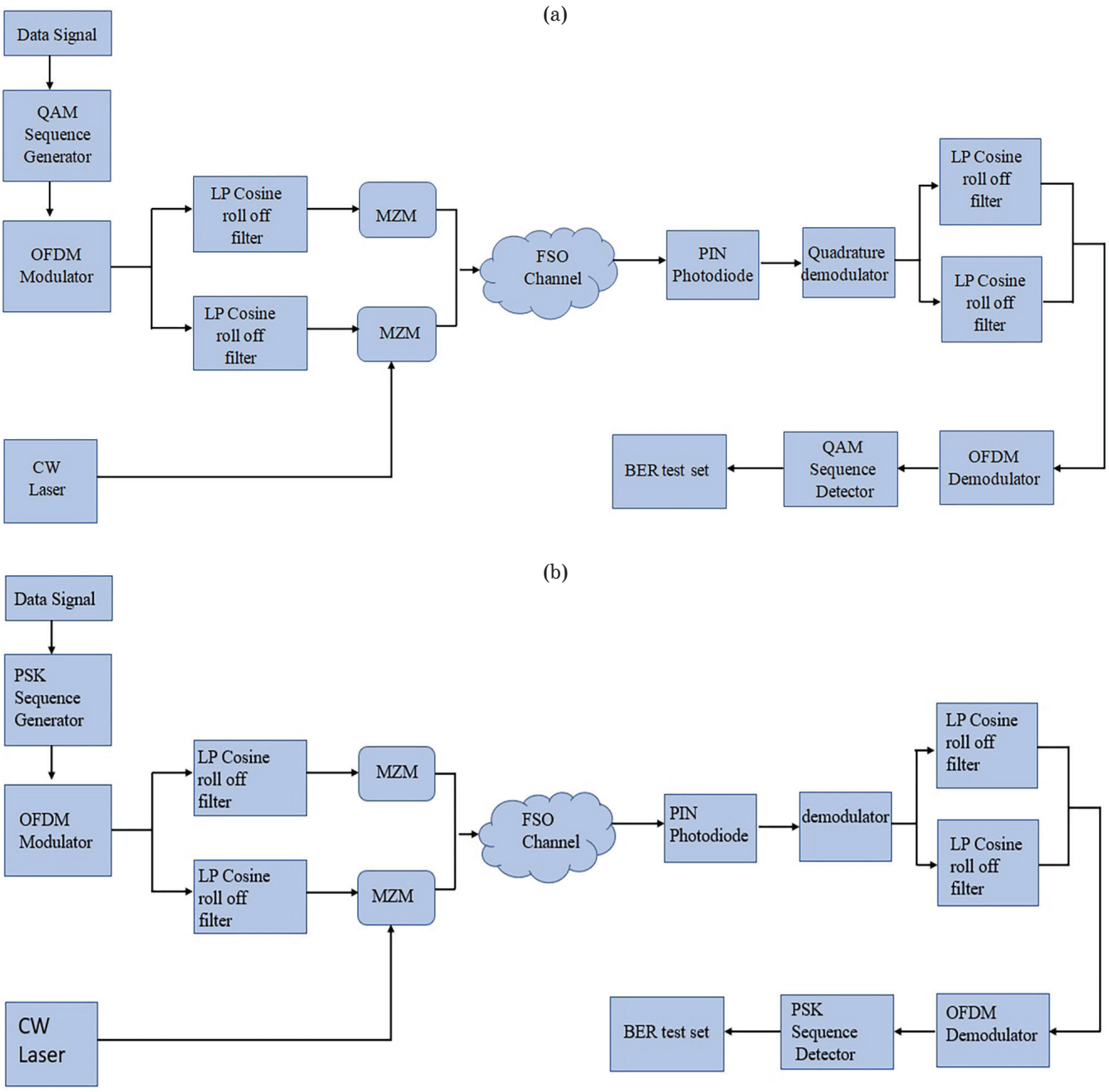

Fig. 6. RoFSO system. (a) 64-QAM-OFDM, (b)16-PSK-OFDM

Рис. 6. Структурная схема RoFSO системы при использовании амплитудной модуляции 64-QAM-OFDM (а), при использованиифазовой двоичной модуляции 16-PSK-OFDM (б)

Cosine roll off filter has been used for pulse-shaping. The transfer function of the filter is given by

$$H(f)=\begin{cases}\alpha, & (f < f_1)\\ 0.5\alpha^2\left[1+\cos\left(\dfrac{f-f_1}{r_p\Delta f_{FWHM}}\pi\right)\right], & (f_1 \le f < f_2)\\ 0, & (f_2 \le f)\end{cases} \quad (5)$$

Here α is the parameter insertion loss, f is the filter frequency, f_c is the filter cutoff frequency, f_{WMM} is full width at half maximum frequency, and r_p is the parameter roll off factor. The parameters f_1 and f_2 are given as

$$f_1 = 1 - r_p f_c \qquad (0 \le r_p \le 1), \tag{6}$$

$$f_2 = 1 + r_p f_c \qquad (0 \le r_p \le 1). \tag{7}$$

In BER analysis the guard bits set in layout parameters act as leading or trailing zero bits. It is calculated in case of single polarization system as

$$\text{BER} = \frac{\text{Errors}}{\text{sequence length} - (2 \times \text{guard bits})}. \tag{8}$$

In case of a dual polarization system the BER is given as

$$\text{BER} = \frac{X\text{Errors} - Y\text{Errors}}{\text{sequence length} - (2 \times \text{guard bits})}, \tag{9}$$

where the Errors are counted only for the portion of the sequence, which is outside the guard bits. The BER is also provided for the X and Y polarization channels as follows:

$$\text{BER}(X) = \frac{X\text{Errors}}{(\text{sequence length} - (2 \times \text{guard bits}))/2}, \tag{10}$$

$$\text{BER}(Y) = \frac{Y\text{Errors}}{(\text{sequence length} - (2 \times \text{guard bits}))/2}. \tag{11}$$

Link margin is expressed as the ratio of received power (P_r) and receiver sensitivity (S) and is given by

$$\text{Link Margin} = \frac{10 \log P_r}{S}. \tag{12}$$

Received power (P_r) is expressed as:

$$P_r = P_t \exp(-\alpha L) \times \frac{A}{(\theta L)^2}, \tag{13}$$

where P_r is the received power, P_t is the transmitted power, A is described as receiver aperture space, θ is defined as divergence angle, α represents region attenuation and L is the distance between receiver and transmitter.

4. SIMULATION RESULTS

In this section simulation results of the proposed RoFSO systems for diverse geographical regions employing 64 QAM and 16 PSK-based OFDM schemes have been investigated. The performance of the proposed RoFSO systems has been evaluated in terms of bit error rate, power received and signal to noise ratio for varying link ranges under rain weather conditions. Optisystem-18 has been used to analyze the system with simulation parameters as depicted in Table 4.

Figure 7 and table 5 depict received power in dBm at the output of RoFSO link for diverse geographical regions of India under the rain weather condition. It can be interpreted from the graph that the received power varies from −26.97 dBm to −42.02 dBm for the coastal region, −26.87 dBm to −40.52 dBm for the hilly region, and −25.99 dBm to −39.12 dBm for the plain region respectively. Thus, received power is the highest for the plain region followed by other two regions. The minimum and the maximum values of the received power of −42.02 dBm and −26.97 dBm respectively have been achieved for different geographic regions.

Figure 8 displays BER versus link range for the RoFSO system. It can be found that the BER varies from 10^{-16} to 10^{-5}, $10^{-21}$to 10^{-9}, and 10^{-24} to 10^{-11}in case of coastal, hilly, and plain

Table 4. Simulation parameters for proposed RoFSO system

Таблица 4. Моделируемые параметры для предложенной системы RoFSO

Simulation parameters	Value
Power of laser source	10 dBm
CW laser wavelength	1550 nm
CW laser power	35 mW
Quadrature modulator frequency	2 GHz
Aperture diameter of transmitter	5 cm
Aperture diameter of receiver	20 cm
No. of subcarriers	1200
Photodetector responsivity	1 A/W
Transmission rate	20 Gbps

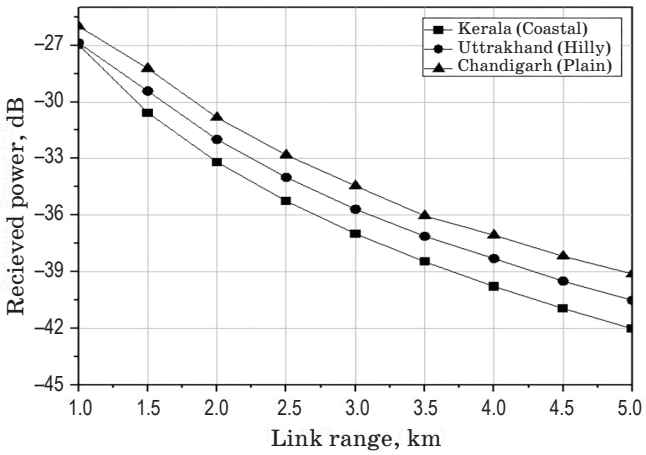

Fig. 7. Received power as a function of link range for different geographic regions employing OFDM based QAM-64 modulation scheme

Рис. 7. Зависимость мощности принимаемого сигнала от дальности связи для различных географических регионов при использовании OFDM со схемой модуляции QAM-64

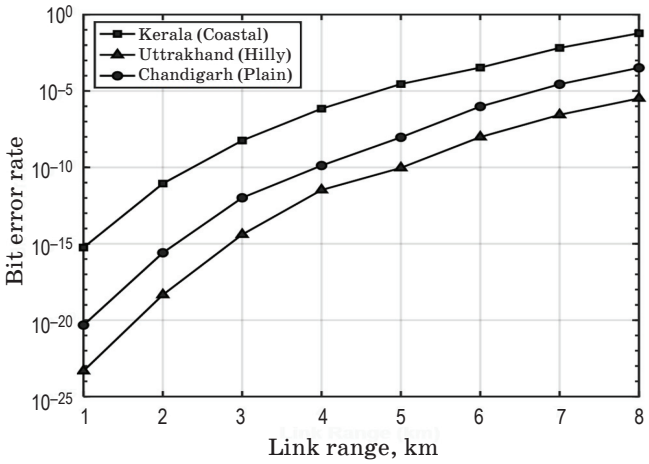

Fig. 8. BER as a function of link range for different geographic regions employing OFDM based QAM 64 modulation scheme

Рис. 8. Зависимость BER от дальности связи для различных географических регионов при использовании OFDM со схемой амплитудной модуляции 64-QAM

Table 5. Received power for different regions employing OFDM based QAM-64

Таблица 5. Мощность принимаемого сигнала для различных географических регионов при использовании OFDM со схемой модуляции QAM-64

Range (Km)	Received power in dBm for different regions		
	Coastal region	Hilly region	Plain region
1	−26.97	−26.87	−25.99
1.5	−30.57	−29.43	−28.23
2	−33.19	−31.99	−30.83
2.5	−35.26	−34.00	−32.81
3	−36.99	−35.69	−34.45
3.5	−38.47	−37.12	−36.04
4	−39.78	−38.3	−37.06
4.5	−40.95	−39.5	−38.18
5	−42.02	−40.52	−39.12

regions respectively considering link range from 1 km to 5 km as listed in Table 6. Minimum BER has been observed in the case of the plain region for a given value of link range. An acceptable value of BER has been achieved up to a transmission range.

Table 6. BER for different regions employing OFDM based QAM-64

Таблица 6. BER для различных географических регионов при использовании OFDM со схемой амплитудной модуляции 64-QAM

Range (Km)	BER for different regions		
	Coastal region	Hilly region	Plain region
1	2.44 e-16	1.12 e-21	1.57 e-24
2	3.88 e-12	1.79 e-16	2.22 e-19
3	4.22 e-9	2.56 e-12	3.42 e-15
4	4.96 e-7	2.67 e-10	4.32 e-12
5	5.78 e-5	4.64 e-9	5.12 e-11
6	6.37 e-4	5.25 e-7	58.3 e-9
7	6.87 e-3	5.85 e-5	6.37 e-7
8	7.66 e-2	8.22 e-4	6.81 e-6

Figure 9 and table 7 depict the SNR in dB at the output of RoFSO link for calculated values of average rain attenuations considering three regions employing OFDM based QAM-64. It can be interpreted from the graph that the SNR varies from 12 to 59.24 dB for the coastal region, 16.23 to 64.43 dB for the hilly region, and 19.55 to 66.93 dB for the plain region respectively. Thus, the highest SNR value is reported for the

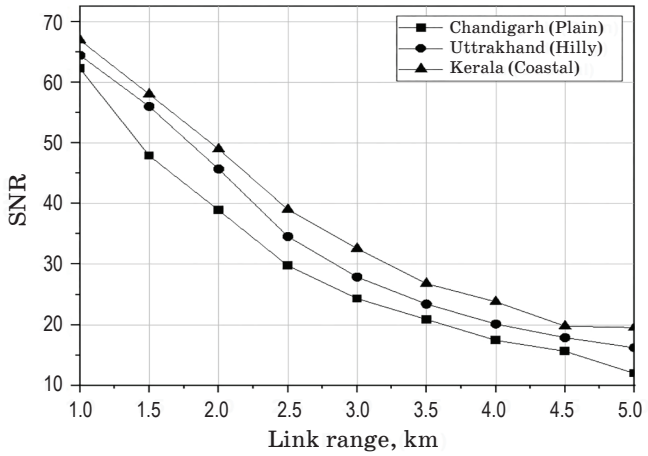

Fig. 9. SNR as a function of link range for different geographic regions employing OFDM based QAM-64 modulation scheme

Рис. 9. Зависимость отношения сигнал/шум от дальности связи для различных географических регионов при использовании OFDMco схемой амплитудной модуляции 64-QAM

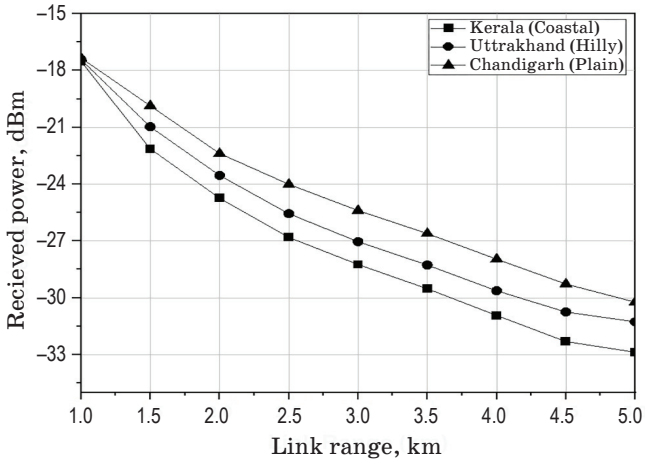

Fig. 10. Received power as a function of link range for different geographic regions employing OFDM based PSK-16 modulation scheme

Рис. 10. Зависимость мощности принимаемого сигнала от дальности связи для различных географических регионов при использовании OFDM на основе схемы фазовой двоичной модуляции 16-PSK

Table 7. SNR for different regions employing OFDM based QAM-64

Таблица 7. Отношение сигнал/шум для различных географических регионов при использовании OFDM со схемой амплитудной модуляции 64-QAM

Range (KM)	SNR in dB for different regions		
	Coastal region	Hilly region	Plain region
1	59.24	64.43	66.93
1.5	47.88	56.00	58.02
2	38.9	45.69	48.98
2.5	29.76	34.56	39.00
3	24.33	27.88	32.56
3.5	20.89	23.43	26.8
4	17.45	20.13	23.79
4.5	15.64	17.89	19.78
5	12.00	16.23	19.55

Table 8. Received power for different regions employing OFDM based PSK-16

Таблица 8. Мощность принимаемого сигнала для различных географических регионов при использовании OFDM на основе схемы фазовой двоичной модуляции 16-PSK

Range (Km)	Received power in dBm for different regions		
	Coastal region	Hilly region	Plain region
1	–17.52	–17.42	–17.34
1.5	–22.13	–20.97	–19.86
2	–24.74	–23.54	–22.38
2.5	–26.81	–25.56	–24.01
3	–28.24	–27.04	–25.39
3.5	–29.52	–28.27	–26.61
4	–30.93	–29.63	–27.96
4.5	–32.31	–30.75	–29.27
5	–32.87	–31.27	–30.23

plain region followed by other two regions for considered transmission range. In case of coastal region, an acceptable value of signal quality is achieved up to a transmission range of 4 km, and longer propagation range may be obtained with higher transmitted power.

Figure 10 and table 8 depict the received power in dBm at RoFSO link output for diverse geographical regions of India under the rain weather condition. It can be interpreted from the graph that the received power varies from –17.52 dBm to –32.87 dBm for the coastal region, –17.42 dBm to –31.27 dBm for the hilly region, and –17.34 dBm

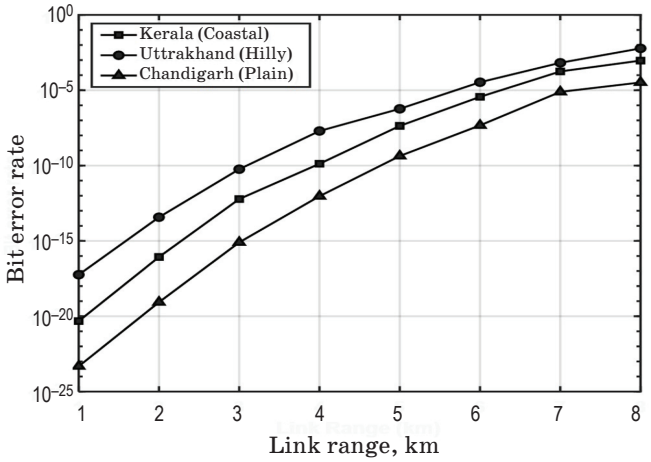

Fig. 11. BER as a function of link range for different geographic regions employing OFDM based PSK-16 modulation scheme.

Рис. 11. Зависимость BER от дальности связи для различных географических регионов при использовании OFDM на основе схемы фазовой двоичной модуляции 16-PSK

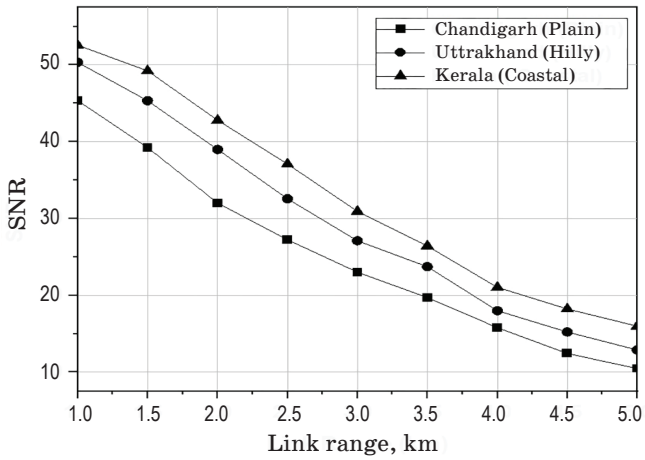

Fig. 12. SNR as a function of link range for different geographic regions employing OFDM based PSK-16 modulation scheme

Рис. 12. Зависимость отношения сигнал/шум от дальности связи для различных географических регионов при использовании OFDM на основе схемы фазовой двоичной модуляции 16-PSK

Table 9. BER for different regions employing OFDM based PSK

Таблица 9. BER для различных географических регионов при использовании OFDM на основе схемы фазовой двоичной модуляции 16-PSK

Range (Km)	BER for different regions		
	Coastal region	Hilly region	Plain region
1	5.77 e-18	9.99 e-21	2.56 e-24
2	1.13 e-14	1.56 e-17	3.87 e-20
3	1.74 e-11	2.71 e-13	1.94 e-16
4	2.34 e-8	2.69 e-10	7.84 e-13
5	2.87 e-7	3.21 e-8	2.43 e-10
6	3.21 e-5	1.99 e-6	2.31 e-8
7	5.36 e-4	2.34 e-4	8.99 e-6
8	8.73 e-3	4.99 e-4	9.85 e-5

Table 10. SNR for different regions employing OFDM based PSK-16

Таблица 10. Отношение сигнал/шум для различных географических регионов при использовании OFDM на основе схемы фазовой двоичной модуляции 16-PSK

Range (Km)	SNR in dB for different regions		
	Coastal region	Hilly region	Plain region
1	45.35	50.33	52.56
1.5	39.23	45.33	49.23
2	32.01	38.98	42.79
2.5	27.22	32.56	37.09
3	23.01	27.09	30.92
3.5	19.69	23.72	26.42
4	15.77	17.98	21.02
4.5	12.43	15.21	18.21
5	10.45	12.87	15.98

to −30.23 dBm for the plain region respectively. Thus, the received power is highest in the flat terrains like plain region followed by other two regions. The minimum and the maximum values of received power of −17.52 dBm to −32.87 dBm respectively have been achieved for different geographic regions.

Figure 11 displays BER versus link range for the RoFSO system. It is found that the BER varies from 10^{-18} to 10^{-7}, 10^{-21} to 10^{-8}, and 10^{-24} to 10^{-9} in case of coastal, hilly and plain regions respectively considering link range from 1 km to 8 km as listed in table 9. Minimum BER has been observed for the plain region for a given value of link range. An acceptable value of BER has been achieved up to a transmission range of 5 km.

Figure 12 and table 10 depict the SNR in dB at the output of RoFSO link for calculated values of average rain attenuations considering three regions employing OFDM based QAM-64. It can be interpreted from the graph that the SNR varies from 10.45 to 45.35 dB for the coastal region, 12.87 to 50.33 dB for the hilly region, and 15.98 to 52.56 dB for the plain region respectively. Thus, the highest value of SNR is reported in the case of plain region followed by other two regions for considered transmission range. In case of coastal region, an acceptable value of signal quality is achieved up to a transmission range of 4 km, and longer propagation range may be obtained with higher value of transmitted power.

The proposed RoFSO system has been evaluated and compared for OFDM based QAM-64 and PSK-16 modulation techniques considering received power, bit error rate, and signal to noise ratio as performance parameters. A higher value of the received power is observed in case of OFDM-QAM-64 as compared to OFDM-PSK-16 scheme for all the considered regions as shown in Fig. 13.

Figures 14 and 15 compare the results in case of two advanced modulation schemes for BER and SNR respectively. RoFSO system employing 64-QAM based OFDM modulation scheme depicts better performance even for the coastal regions,

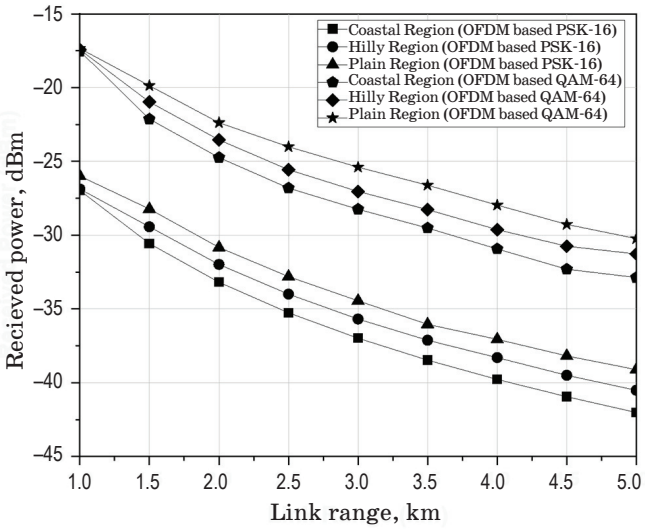

Fig. 13. Received power employing OFDM based QAM-64 and PSK-16

Рис. 13. Сравнение принимаемой мощности при использовании OFDM со схемами с амплитудной модуляцией 64-QAM и фазовой двоичной модуляцией 16-PSK

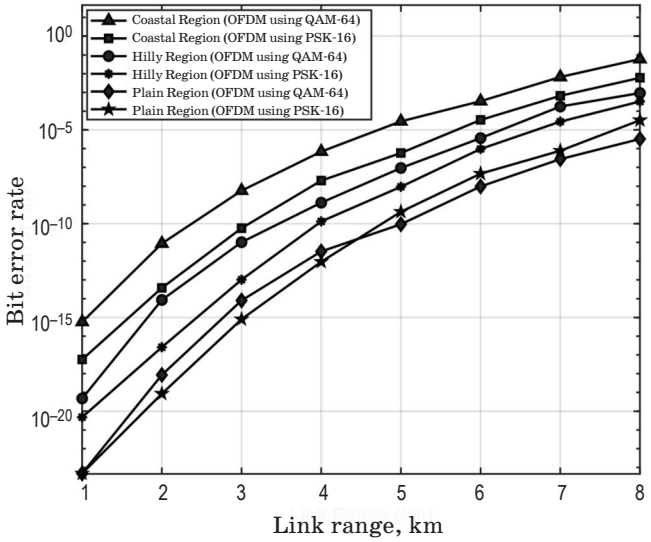

Fig. 14. BER employing OFDM based QAM-64 and PSK-16

Рис. 14. Сравнение BER при использовании OFDM со схемами с амплитудной модуляцией 64-QAM и фазовой двоичной модуляцией 16-PSK

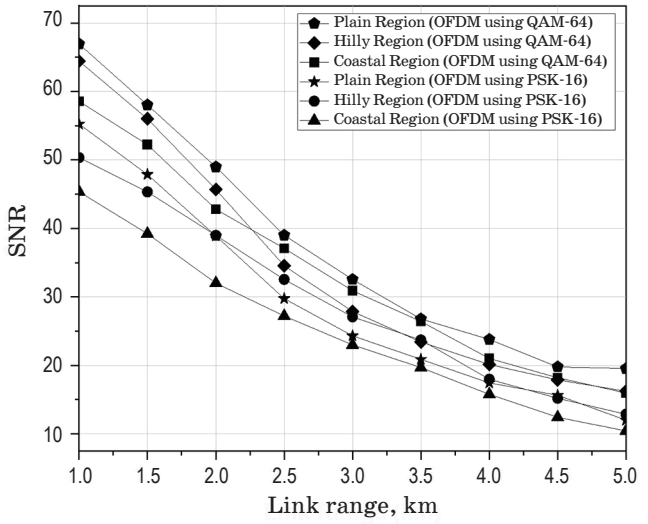

Fig. 15. SNR employing OFDM based QAM-64 and PSK-16

Рис. 15. Сравнение отношения сигнал/шум при использовании OFDM со схемами с амплитудной модуляцией 64-QAM и фазовой двоичной модуляцией 16-PSK

which experience heavy rainfall. An increased value of SNR of 2 to 17 dB have been observed in this case by employing QAM-64 scheme as compared to PSK-16 over the considered transmission range (Fig.15). Similarly, the achievement of better BER values over longer distances

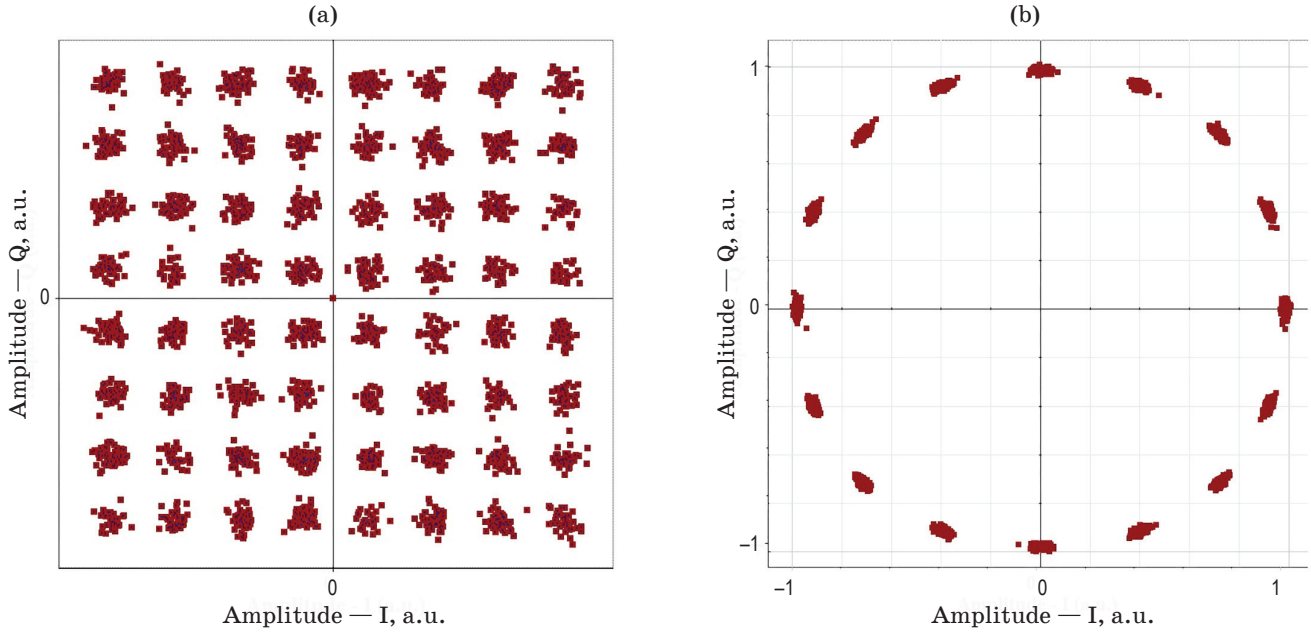

Fig. 16. Constellation plots at the receiver's side of the propose dRoFSO system (a) OFDM based QAM-64, (b) OFDM based PSK-16

Рис. 16. Диаграммы направленности принимаемого сигнала систем RoFSOпри использованииOFDM на основе QAM-64 (a), при использовании OFDM на основе PSK-16(б)

Table 11. Comparison of proposed work with previous works
Таблица 11. Сравнение полученных результатов исследований с результатами других авторов

Parameters	[22]	[23]	[24]	[25]	[26]	Proposed work
Modulation type	Not specified	NRZ based OOK	NRZ based AM	Not specified	RZ- DPSK based WDM	64-QAM and 16-PSKbased OFDM
Authentic meteorological data	No	Malaysian meteorological department	No	No	No	Yes
Geographical region	Tropical	Coastal	Not specified	Tropical	Not specified	Coastal, plain and hilly
Maximum link range	0.8 km	2.5 km	1.9 km	3 km	3 km	6 km
Data rate (Gbps)	1	2	10	Not specified	80	20
Type of system	FSO	FSO	RoFSO	FSO	FSO	RoFSO

concludes that OFDM based QAM-64 is best suited specially for applications in coastal areas.

Figures 16a and 16b depict the constellation plots of the 64-QAM and 16-PSK based OFDM RoFSO system respectively to ascertain the quality of the received signal. Table 11 outlines the comparison of the proposed work with the previous works in literature. Real time rain rate data analysis of diverse geographical regions with the achievement of higher transmission

range employing advanced modulation technique ensures the enhanced performance of the proposed RoFSO system as compared to other related work.

5. CONCLUSION

In this work the rain attenuation has been investigated for analyzing RoFSO system performance for diverse topography of India. A real-time rain rate analysis of the monsoon months for the years ranging from 2014 to 2020 has been evaluated using Marshal and Palmer rain attenuation model. The results have been investigated for bit error rate, received power, and SNR for varying channel link range employing OFDM based QAM-64 and PSK-16 modulation formats. An acceptable value of BER of 10^{-9} is achieved over the transmission range of 3, 5 and 6 km for coastal, hilly and plain regions respectively. 64-QAM based OFDM modulation scheme depicts better performance even for the coastal regions, which experience heavy rainfall, and a higher value of SNR of 2 to 17 dB has been observed over the transmission range of 1 to 5 km.

In future real-time data analysis of different atmospheric turbulence conditions may be carried out for RoFSO system employing the advanced modulation technique for the next generation data services, such as 6G. The proposed system may find its application for deployment in smart cities and seamless wireless connectivity among the diverse terrains with varying weather conditions.

REFERENCES

1. Amphawan A., Chaudhary S., Neo T.K., Kakavand M., Dabbagh M. Radio-over-free space optical space division multiplexing system using 3-core photonic crystal fiber mode group multiplexers // Wireless Networks. 2021. V. 27. № 1. P. 211–225.https://doi.org/10.1007/s11276-020-02447-4
2. Zhang Z., Xiao Y., Ma Z. 6G wireless networks vision, requirements, architecture, and key technologies // IEEE Vehicular Technology Magazine.2019. V. 14. № 3. P. 28–41. http://doi: 10.1109/MVT.2019.2921208
3. Esmail M.A., Fathallah H., Alouini M.-S. Outdoor FSO communications under fog: Attenuation modeling and performance evaluation // IEEE Photonics Journal. 2016. V. 18. №8(4). P. 1–22.http://doi:10.1109/JPHOT.2016.2592705.
4. Ullah H., Nair N.G., Moore A., Nugent C. et al. 5G communication: An overview of vehicle-to-everything, drones, and healthcare use-cases // IEEE Access. 2019. P. 1-1. https://doi.org/ 10.1109/ACCESS.2019.2905347
5. Hamza A.S., Deogun J.S., Alexander D.R. Classification framework for free space optical communication links and systems // IEEE Communications Surveys & Tutorials.2019. V. 21. № 2. P. 1346–1382. https://doi.org/ 10.1109/COMST.2018.2876805
6. Singh H., Mittal N., Miglani R., Singh H., Gaba G.S., Hedabou M. Design and analysis of high-speed free space optical (FSO) communication system for supporting Fifth Generation (5G) data services in diverse geographical locations of India // IEEE Photonics Journal.2021. V. 13. № 5. P. 1–12. Oct. Art no. 7300312. https://doi.org/ 10.1109/JPHOT.2021.311365
7. Kumar A., Krishnan P. RoFSO system based on BCH and RS coded BPSK OFDM for 5G applications in smart cities // Optical and Quantum Electronics. 2022.V. 54(1). P. 1–6. https://doi.org/10.1007/s11082-021-03392-y
8. Sabu S., Renimol S., Abhiram D., Premlet B. Effect of rainfall on cellular signal strength: A study on the variation of RSSI at user end of smartphone during rainfall // 2017 IEEE Region 10 Symposium. 2017. P. 1–4. https://doi.org/ 10.1109/TENCONSpring.2017.8070024
9. Alheadary W.G., Park K.H., Alfaraj N., Guo Y. Free-space optical channel characterization and experimental validation in a coastal environment // Optics Express. 2018. V. 26(6). Mar 19. P. 6614–28. https://doi.org/10.1364/OE.26.006614
10. Alnajjar S.H., Jasim Hadi M. The effect of atmospheric turbulence on the performance of end-users antenna based on WDM and hybrid amplifier // 2021 3rd International Conference on Electronics Representation and Algorithm (ICERA). 2021. P. 23–28.https://doi.org/10.1109/ICERA53111.2021.9538655
11. Grover A., Sheetal A. A cost-effective high-capacity OFDM based RoFSO transmission link incorporating hybrid SS-WDM-MDM of Hermite Gaussian modes // Optoelectronics and Advanced Materials Rapid Communications. 2020. Apr 9. 14. March–April. P. 136–45. https://oam-rc.inoe.ro/articles/a-cost-effective-high-capacity-ofdm-based-rofso-transmission-link-incorporating-hybrid-ss-wdm-mdm-of-hermite-gaussian-modes/fulltext
12. Kolev D.R., Wakamori K. Transmission analysis of OFDM-Based services over line-of-sight indoor infrared laser wireless links // J. Lightwave Technol. 2021. V. 30. P. 3727–3735. https://doi: 10.1109/JLT.2012.2227456
13. Singh M., Malhotra J. Performance comparison of M-QAM and DQPSK modulation schemes in a 2×20 Gbit/s–40 GHz hybrid MDM–OFDM-based radio over FSO transmission system // Photonic Network Communications. 2019. V. 38(3). Dec. P. 378–89. https://doi.org/10.1007/s11107-019-00861-z
14. Prabu K., Utsav J., Balaji Ka. Asymptotic BER analysis of QAM and PSK with OFDM RoFSO over M — turbulence in the presence of pointing errors // IET Communications. 2018. V. 12. P. 2046–2051. https://doi.org/10.1049/iet-com.2017.0560
15. Siegel T., Chen S.P. Investigations of free space optical communications under real-world atmospheric conditions // Wireless Personal Communications. 2021. V. 116(1). P. 475–90. https://doi.org/10.1007/s11277-020-07724-1
16. Gadze J.D., Akwafo R., Affum E.A. Analysis of 75 GHz millimeter wave radio over fiber-based fronthaul

system for future networks // International Journal of Advanced Research in Computer and Communication Engineering. 2020. V. 9(4). P. 79–95. https://doi.org/10.17148/IJARCCE.2020.9415
17. Ninos M.P., Nistazakis H.E., Leitgeb E., Tombras G.S. Spatial diversity for QAM OFDM RoFSO links with nonzero boresight pointing errors over atmospheric turbulence channels // Journal of Modern Optics. 2018. V. 66(3). P. 241–251 https//doi.org/: 10.1080/09500340.2018.1516828
18. Kaur S., Tabassum N. // IETE Journal of Research. 2021. V. 69(4). P. 1934–1944. https://doi.org/ 10.1080/03772063.2021.1878067
19. Sharma A., Kaur S. Performance evaluation and fog attenuation modelling of FSO link for hilly regions of India // Opt. Quant. Electron.2021. V. 53. P. 697. https://doi.org/10.1007/s11082-021-03348-2
20. Sharma A., Kaur S. Performance analysis of 1280 Gbps DWDM – FSO system employing advanced modulation schemes // Optik. 2021. V. 248. P. 168135. https://doi.org/10.1016/j.ijleo.2021.168135
21. Sharma A., Kaur S., Chaudhary S., Sushank. Performance analysis of 320 Gbps DWDM—FSO System under the effect of different atmospheric conditions // Optical and Quantum Electronics. 2021. V. 53. P. 239. https://doi.org/10.1007/s11082-021-02904-0
22. Ali A. Mazin. Analysis study of rain attenuation on optical communications link // International Journal of Engineering. Business and Enterprise Applications (IJEBEA). 2013. № 6. P. 18–24.
23. Rahman A.K., Julai N. Impact of rain weather over free space optic communication transmission// Indonesian Journal of Electrical Engineering and Computer Science. 2019. V. 14. P. 303–310. https://doi.org/10.11591/ijeecs.v14.i1.pp303-310
24. Adnan S.A., Ali M.A.A., Al-Saeedi S.A. Characteristics of RF signal in free space optics (RoFSO) considering rain effect // Journal of Engineering and Applied Sciences. 2018. V. 13(7). P. 1644-8. 10.39https://doi.org/23/jeasci.2018.1644.1648
25. Basahel A.A., Islam M.R., Zabidi S.A. Availability assessment of free-space-optics links with rain data from tropical climates // Journal of Lightwave Technology. 2017. Oct 1. V. 35(19). P. 4282-8. https://doi.org/ 10.1109/JLT.2017.2732459
26. Badar N., Jha R.K., Towfeeq I. Performance analysis of an 80 (8×10) Gbps RZ-DPSK based WDM-FSO system under combined effects of various weather conditions and atmospheric turbulence induced fading employing Gamma–Gamma fading model // Optical and Quantum Electronics. 2018. V. 50. № 1. P. 1–11. https://doi.org/10.1007/s11082-017-1306-y

AUTHORS

Sanmukh Kaur — PhD, Associate Professor, Amity University, 201303, Noida, India; Scopus ID:55233637600, https://orcid.org/0000-0002-1750-5684, sanmukhkaur@gmail.com

Jasleen Kaur — M.Tech, Student, Amity University, 201303, Noida, India; https://orcid.org/0000-0001-5576-9149, jasleen_kaur@outlook.in

The article was submitted to the editorial office 15.04.2022
Approved after review 20.10.2022
Accepted for publication 26.06.2023

Статья поступила в редакцию 15.04.2022
Одобрена после рецензирования 20.10.2022
Принята к печати 26.06.2023